Synthesis and characterization of electrospun LiNbO3 nanofibers

M.C. Maldonado-Orozco, M.T. Ochoa-Lara, J.E. Sosa-Márquez, S.F. Olive-Méndez, **F. Espinosa-Magaña**

Abstract

Lithium niobate nanofibers were synthesized by the electrospinning method after heat treatment of composite nanofibers of polyvinylpyrro-lidone (PVP), niobium ethoxide and lithium hydroxide, dissolved in ethanol. The thermal stability, morphology, microstructure and crystal structure of as-spun composite and calcined nanofibers were characterized by thermogravimetric analysis (TGA), differential scanning calorimetry (DSC), scanning electron microscopy (SEM), X-ray diffractometry (XRD), transmission electron microscopy (TEM) and Raman spectroscopy. The size and morphology of the calcined nanofibers are strongly affected by the high voltage applied during the electrospinning process. With 8 kV, fibers with diameter around 100–300 nm were obtained, while at an applied voltage of 15 kV, some necklace-like structures were synthesized, formed by irregular shaped nanoparticles with sizes in the range of 60–160 nm.

Keywords: Lithium niobate; Nanofibers; Electrospinning

1. Introduction

Ferroelectric oxides ABO3 where A is an alkali or rare-earth element, and B represents a transition metal, such as LiNbO3, are widely used in the fields of nonlinear optics, pyroelectric detectors, electro-optical modulators, thin-film capacitors, and optical memories [1]. Lithium niobate occurs in two phases of trigonal symmetry with ten atoms per unit cell. The ground-state is ferroelectric with space group R3c. It has advantages over most other ferroelectric materials, as it is thermally, mechanically and chemically stable and also possesses a small dielectric

constant. Because its properties are dependent not only on its chemical composition but also on its structure, shape and size, it has been found that reduction of the grain size to the nanoscale leads to distinct and frequently enhanced properties compared to those of the bulk. Over the last few decades, one dimensional nano materials such as nanotubes and nanofibers have attracted great attention due to their unique structure and properties, i.e. large specific surface area and chemical/mechanical stabilities. Thus nanofibers can be used as building blocks in nanotechnology [2]. Over the past decades, several ceramic nanostructures have been synthesized by various processes, e.g. solution method, laser ablation and chemical vapor deposition. Recently, there has been an intense research effort on electro-spinning of ceramics since it is a straightforward way to synthesize nanostructures. Although some metal oxide nano-fibers, e.g., TiO2 [3],SnO2 [4],V2O5 [5],and ZnO [6],aswell as ceramic compounds, e.g., NiCo2O4 [7],MgTiO [8], among many others, have been successfully synthesized by electrospinning process, followed by calcination at high temperature, we were not able to find any reports on the synthesis of lithium niobate nanofibers by the electrospinning technique, while we did find some articles on the synthesis of lithium niobate nanostructures, e.g., nanoparticles [10,11], nanowires [12,13] and microtubes [14].

2. Experimental

The synthesis of LiNbO3 nanofibers was carried out by the electro-spinning method. A detailed description of the procedure can be found in the literature [9]. In this work, the precursor solution was composed of poly (vinylpyrrolidone) (PVP), niobium ethoxide (Nb (OCH2CH3)5) and lithium hydroxide (LiOH), dissolved in

ethanol. The solution was heated at 30 °C with stirring for 4 h and then delivered into a metallic needle at a constant flow rate of 0.3 mL/h by a syringe pump. The metallic needle was connected to a high-voltage power supply and a grounded aluminum foil was placed 15 cm from the needle tip. Two voltages were applied in the electrospinning process, namely 8 and 15 kV, producing an electric field of 5.3 x 10^4 and 1 x 10^5 V/m, respectively. The precursor solution jet was accelerated toward the aluminum foil, leading to the formation of Nb(OCH2CH3)5/LiOH/PVP composite fibers, together with a rapid evaporation of the ethanol.

In order to determine the annealing temperature to reach the desired LiNbO3 compound, the thermal stability of as-spun Nb (OCH2CH3)5/LiOH/PVP composite was analyzed by thermogravimetry-differential scanning calorimetry (TGA–DSC) using a TA Instruments SDT Q600 thermal analyzer at a heating rate of 10 °C/min under inert atmosphere with 50 cm3/min of Argon flux.

X-ray diffraction (XRD) measurements were performed in a Panalytical diffractometer with Cu Kα1 radiation (1.540598 Å). For XRD measurements, the nanofibers were separated from the aluminum foil and then slightly pressed on a glass slide to form a dense film. Field-emission scanning electron microscopy (FESEM) images were acquired with a JEOL JSM-7401F, at an accelerating voltage of 5 kV. High-resolution transmission electron microscopy (HRTEM) images were acquired by using a JEOL JEM-2200FS microscope.

Further material identification was conducted by acquiring Raman spectra with a LabRam Horiba HR system, using a 632.8 nm He–Ne laser at 14.2 mW, equipped with a column of CCD detectors cooled at -75 °C, with a resolution of

about $1cm^{-1}$.

Raman scattering is sensitive to impurities, stoichiometry and strain, so its capability to probe material symmetry allows not only for material identification but also for the determination of the crystallographic phase, where even very small displacements affect the Raman selection rules.

3. Results and discussion

The thermogravimetric analysis and differential scanning calorimetry (TGA DSC) results are shown in Fig. 1. The TGA profile reveals that evaporation of residual molecules of ethanol, as well as that due to the OH radical from lithium hydroxide, are responsible for the mass loss at T <180 °C and confirmed by the endothermic peak appearing around 100 °C in the DSC curve. Two additional losses are observed above 180 °C that can be interpreted with the aid of the DSC analysis. Two peaks, centered approximately at 320 °C and 420 °C dominate the DSC profile. They indicate the occurrence of exothermic reactions. The peak at the lower temperature is attributable to the decomposition of the acetate group, whereas the one at the higher temperature is likely originated from the breakdown of the polymer backbone. On this basis, we chose 600 1C and 700 1C as suitable temperatures for calcinations of the as-spun fibers. However, XRD showed that nanofibers obtained from calcination at 600 °C did not reach the desired crystallographic phase, because some residual parts of the polymer are still present, even when the slope of the TGA curve is almost zero. Only at 700 °C, was the presence of pure trigonal phase of LiNbO3, as confirmed by XRD analysis.

Fig. 2 shows XRD patterns from the amorphous structure (as-spun) and calcined LiNbO3 fibers, showing the formation of crystalline lithium niobate. Diffraction-peak identification is performed on the basis of the PDF2 release 2010 ICDD database, card number 00-020-0631.

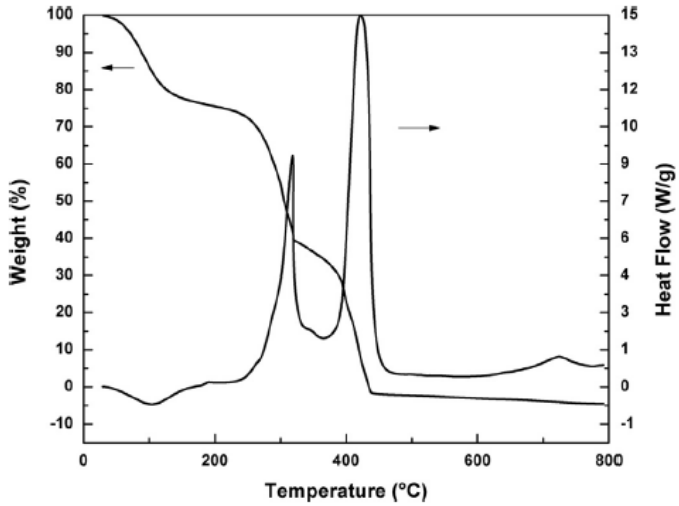

Fig. 1. TGA–DSC analysis of as-spun $Nb(OCH_2CH_3)_5$/LiOH/PVP fiber composite.

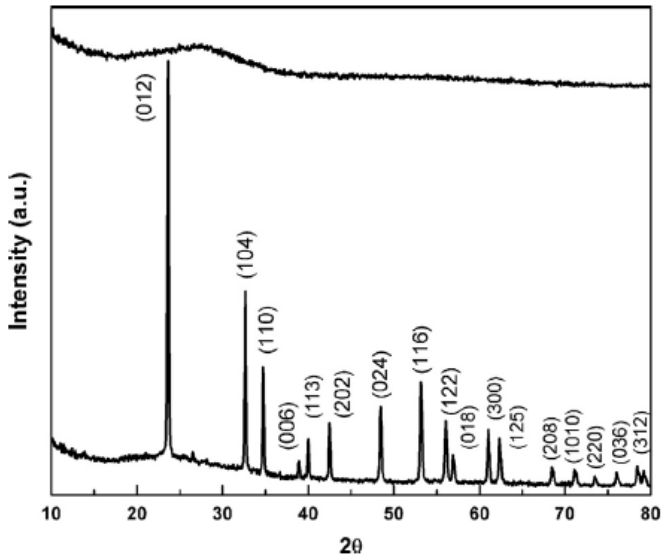

Fig. 2. XRD patterns of as-spun and calcined $Nb(OCH_2CH_3)_5$/ LiOH/PVP composite.

Fig. 3a and b shows SEM micrographs of as-spun fibers, obtained at 8 kV and 15 kV, respectively. Cylindrical and randomly oriented Nb(OCH2CH3)5/LiOH/PVP composite fibers were obtained with diameters in the range 97–247 nm for 8 kV and 94–180 nm for 15 kV. Fig. 4a and b shows TEM micrographs from calcined LiNbO3 nanofibers, after dispersion of the sample in isopropanol. Fig. 4a shows fibers obtained at 8 kV, with two different diameters of 115 and 235 nm, whereas Fig. 4b shows necklace-like nanofibers, formed by irregular shaped nanoparticles with sizes between 60 and 160 nm. A high resolution micrograph, taken from a single nanoparticle composing the fiber is shown in the inset of Fig. 4b, where well-defined planes are observed, indicating a good crystallinity of the nanoparticles. The two lattice planes observed can be ascribed to lattice spacing of 0.261 nm and 0.201 nm, corresponding to the (110) and (202) planes of the rhombohedral phase of LiNbO3.

The Raman spectrum of the electrospun nanofibers at 8 kV and calcined at 700 °C in the spectral range of 100–900 cm^{-1} is shown in Fig. 5, together with the spectrum obtained from commercial LiNbO3 powder (Sigma-Aldrich, 99.9% purity), for comparison. Peaks observed at 153 (151), 237 (240), 369 (370) and 583 (585) cm^{-1}in commercial (nanofibers) samples correspond to the strongest characteristic E transverse optical (TO) phonon modes of LiNbO3, consistent with a hexagonal ferroelectric phase [15]. The strongest fundamental A1 TO mode, expected at 630cm^{-1}, has been shifted to a lower wavenumber of 613 (622) cm^{-1} for commercial (nanofibers) Sample. Similarly, the peak observed at 876 (875)cm^{-1}, expected at 883cm^{-1}, can be assigned to the quasi TO mode.

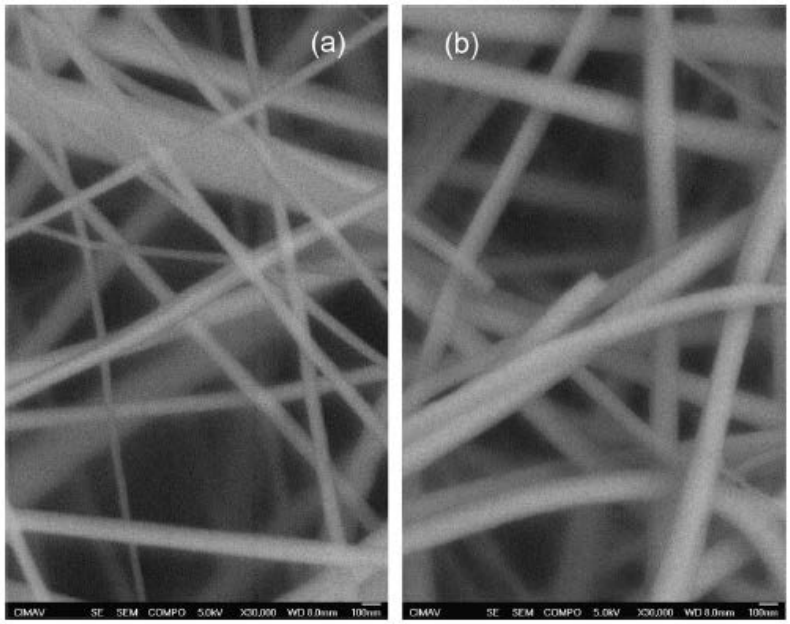

Fig. 3. SEM images of as-spun $Nb(OCH_2CH_3)_5$/LiOH/PVP composite. (a) at 8 kV and (b) at 15 kV.

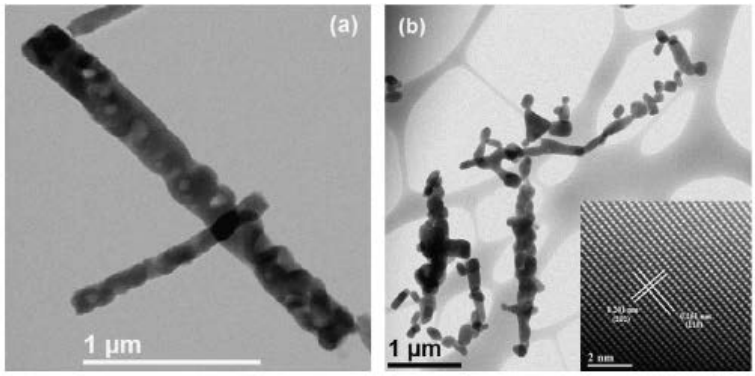

Fig. 4. TEM images of $LiNbO_3$ nanofibers. (a) cylindrical nanofibers obtained at 8 kV and (b) necklace-like nanofibers obtained at 15 kV. The inset graph shows a high resolution micrograph from a nanoparticle from the necklace-like nanofibers.

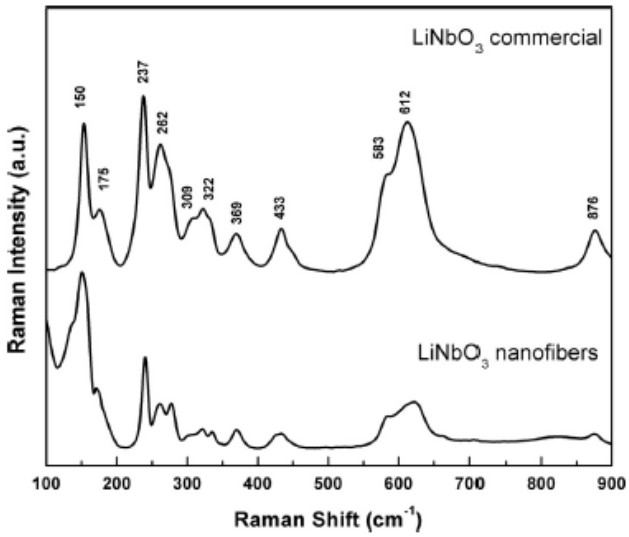

Fig. 5. Raman spectra of $LiNbO_3$ necklace-like nanofibers, obtained at 8 kV and commercial powder.

4. Conclusions

Lithium niobate nanofibers with trigonal crystal structure were synthesized by electrospinning, using poly(vinylpyrroli-done), niobium ethoxide and lithium hydroxide, as starting precursor solution. Electrospun nanofibers composites were acquired at two high-voltage values of 8 kV and 15 kV, giving rise to nanofibers with two different morphologies, cylindrical and necklace-like nanofibers of polycrystalline lithium niobate, after annealing at 700 °C for 6 h. Necklace-like nanofibers are composed of irregular polyhedron shaped nanoparticles with dimensions around 60–160 nm and a few mm in length, with good crystallinity, as seen in atomic-resolution transmission electron microscopy. Raman spectroscopy confirms the hex-agonal character of the fibers.

Acknowledgments

Technical support of Carlos Ornelas, Wilber Antúnez, Enrique Torres and

Daniel Lardizábal is greatly appreciated. One of the authors (M.C. Maldonado-Orozco) gratefully acknowledges the support grant from CONACYT, Mexico (Grant no. 210558).

References

[1] Y. Xu, Ferroelectric Materials and Their Applications, North-Holland, Amsterdam, 1991.

[2] Y. Dzenis, Spinning continuous fibers for nanotechnology, Science 304 (2004) 1917–1919.

[3] K.C. Sung, K. Soonhyun, K.L. Sang, P. Hyunwoong, Photocatalytic comparison of TiO2 nanoparticles and electrospun TiO2 nanofibers: effects of mesoporosity and interparticle charge transfer, J. Phys. Chem. 114 (2010) 16475–16480.

[4] X. Xin, L. Shuli, W. Xin, L. Junxiong, W. Qufu, Z. Xiangwu, Structures and properties of SnO2 nanofibers derived from two different polymer intermediates, J. Mater. Sci. 48 (2013) 3378–3385.

[5] D.M. Carrillo-Flores, M.T. Ochoa-Lara, F. Espinosa-Magaña, Electron energy-loss spectroscopy of V2O5 nanofibers synthesized by electro-spinning, Micron 52 (2013) 39–44.

[6] W. Hui, W. Pan, Preparation of zinc oxide nanofibers by electrospinning,

J. Am. Ceram. Soc. 89 (2006) 699–701.

[7] H. Guan, S. Changlu, L. Yichun, Y. Na, Y. Xinghua, Fabrication of NiCo2O4 nanofibers by electrospinning, Solid State Commun. 131 (2004) 107–109.

[8] S. Aryal, N. Dharmaraj, S.R. Bhattarai, M.S. Khil, H.Y. Kim, Deposition of gold nanoparticles on electrospun MgTiO3 ceramic nanofibers,

J. Nanosci. Nanotechnol. 6 (2006) 510–513.

[9] S. Sharma, Ferroelectric nanofibers: principle, processing and applications, Adv. Mater. Lett. 4 (2013) 522–533.

[10] M. Niederberger, N. Pinna, J. Polleux, M. Antonietti, A general soft-chemistry route to perovskites and related materials: synthesis of BaTiO3, BaZrO3, and LiNbO3 nanoparticles, Angew. Chem. Int. Ed. 43 (2004) 2270–2273.

[11] F. Johann, T. Jungk, S. Lisinski, A. Hoffmann, L. Ratke, E. Soergel, Sol–gel derived ferroelectric nanoparticles investigated by piezoresponse force microscopy, Appl. Phys. Lett. 95 (2009) 202901.

[12] R. Grange, J.W. Choi, C.L. Hsieh, Y. Pu, A. Magrez, R. Smajda,

L. Forró, D. Psaltis, Lithium niobate nanowires synthesis, optical properties, and manipulation, Appl. Phys. Lett. 95 (2009) 143105.

[13] K. Saito, K. Koga, A. Kudo, Lithium niobate nanowires for photocatalytic water splitting, Dalton Trans. 40 (2011) 3909–3913.

[14] L. Zhao, M. Steinhart, M. Yosef, S.K. Lee, T. Geppert, E. Pippel,

R. Scholz, U. Gösele, S. Schlecht, Lithium niobate microtubes within ordered macroporous silicon by templated thermolysis of a single source precursor, Chem. Mater. 17 (2005) 3–5.

[15] A.C. Santulli, H. Zhou, S. Berweger, M.B. Raschke, E. Sutterc, S.S. Wong, Synthesis of single-crystalline one-dimensional LiNbO3 nanowires, CrystEngComm 12 (2010) 2675–2678.